**Supporting Information**

# A Simple Way to Finely Tune the Redox Potentials of Cobalt Ions Encapsulated in Nitrogen Doped Graphene Molecular Catalysts for Oxygen Evolution Reaction

*Jiong Wang*[1], *Wen-Feng Lin*[2], *Yi Shi*[1], *Huai-Song Wang*[1], *Lian-Qing Rong*[3]* and *Xing-Hua Xia*[1]*

[1]State Key Laboratory of Analytical Chemistry for Life Science and Collaborative Innovation Center of Chemistry for Life Sciences, School of Chemistry and Chemical Engineering, Nanjing University, Nanjing 210093, China.
[2]Department of Chemical Engineering, Loughborough University, Loughborough, Leicestershire, LE11 3TU, U.K.
[3]Department of Materials and Chemical Engineering, Pingxiang University, Pingxiang 337055, China
E-mail: xhxia@nju.edu.cn (X.H. Xia) and lqrong2021@163.com (L. Q. Rong)

## Experiments

**Reagents and Apparatus.** The Graphite precursor (99.9995%, 100 mesh) was purchased from Alfa Aesar Company. Metal chlorides, cobalt salts and other reagents were of analytical-reagent grade. All aqueous solutions were prepared using Millipore water with resistivity of 18.2 MΩ•cm. The morphologies of the prepared catalysts were characterized by transmission electron microscopy (TEM, JEM-2100, JEOL Company, Japan). The Raman spectra were carried out on a FT-Raman Spectrometer (Bruker Company, German). X-ray diffraction pattern was carried out on a X'TRA spectrometer (Switzerland). XPS survey were obtained on a PHI 5000 VersaProbe (UlVAC-PHI Company, Japan), and curve fitting of elemental fine spectra were performed using 20% Gaussian-Lorentzian peak shape. Atomic absorption spectroscopy was performed to measure the cobalt content in the catalysts (180-80 type, Hitachi Company, Japan).

**Synthesis of Transition Metal Ions-Nitrogen Doped Graphene Catalysts.** Graphite oxide (GO) was prepared according to the method reported previously. GO was mixed with melamine in aqueous solution at a mass ratio of 1: 10 (GO: Melamine). The resultant suspension was then quickly immersed into liquid nitrogen to grow ice crystal template, afterwards the hybrid was sublimated under vacuum below 0 °C. The dried hybrid was annealed at 800 °C in Ar atmosphere for 1 h to achieve nitrogen doped graphene (NG). The NG was further mixed with different metal ions (chloride salts of $Mn^{2+}$, $Fe^{2+}$, $Co^{2+}$, $Ni^{2+}$, $Zn^{2+}$ and $Cu^{2+}$ ions) in $CH_3OH$ at room temperature for 12 h, forming the final electrocatalysts (NG-M) which were further washed with EtOH for several times and then dried at room temperature. The electrocatalysts with different counter anions of $Co^{2+}$ ions on NG (NG-Co-L) were synthesized by using the same methods as for NG-Co but by using different cobalt salts as precursors.

**Electrochemical Measurements.** Rotating ring disk electrode (RRDE, PINE Inc, USA) was applied to assess the OER and ORR performance on different catalysts. Typically, the disk (glassy carbon, 5.61 mm in diameter) was casted with 6 μL catalyst suspensions (1 mg $mL^{-1}$/ EtOH) as the working electrode, Ag/AgCl electrode and Pt wire were used as the reference and counter electrodes, respectively. The collection efficiencies (N) of each modified disk electrode was measured in 1 mM $Fe(CN)_6^{3+}$/0.1 M KCl electrolyte. The apparent electron number (*n*) of ORR was calculated in terms of the equation ($n = 4\ i_d / (i_d + i_r/N)$) as previously reported. The potentiostat used in this work was CHI 900D (CH Instrument Inc., USA). For electrocatalytic measurements of ORR and OER, the potentials *vs.* Ag/AgCl electrode were converted to the values referring to reversible hydrogen electrode (RHE). In 0.1 M KOH, the open circuit potential keeps at about 0.95 V (E(RHE) = E (Ag/AgCl) + 0.95 V).

TOFs of Co site was calculated in terms of the equation:

$$\mathrm{TOF} = (J \times A)/(4 \times F \times m),$$

where $J$ stands for the anodic current density, $A$ stands for the electrode surface area, $F$ is Faraday constant (96485 C $mol^{-1}$) and $m$ is the mole amount of $Co^{2+}$ ions. For TOF calcuation, $m$ was determined by the charge amount of $Co^{2+/3+}$ couple of CVs. For minimum TOF calculation, $m$ was determined by the atomic absorption spectroscopy (AAS) measurement.

***An in situ* Fluorescence Spectroelectrochemistry.** Using a typical three-electrode system, the electrocatalysis of OER and ORR on a GC electrode (3 mm in diameter) modified with 1 μL catalysts suspension in KOH was performed on a CHI 660D potentiostat (CH Instrument Inc., USA). A 60 μM signal probe of coumarin was added into the KOH electrolyte. The fluorescence variation was recorded on a RF-5301PC fluorescence spectrophotometer (Shimadzu, Japan) during OER and ORR. The concentration of KOH electrolyte was diluted to 0.01 M for avoiding hydrolysis of coumarin.[1]

## Additional Results

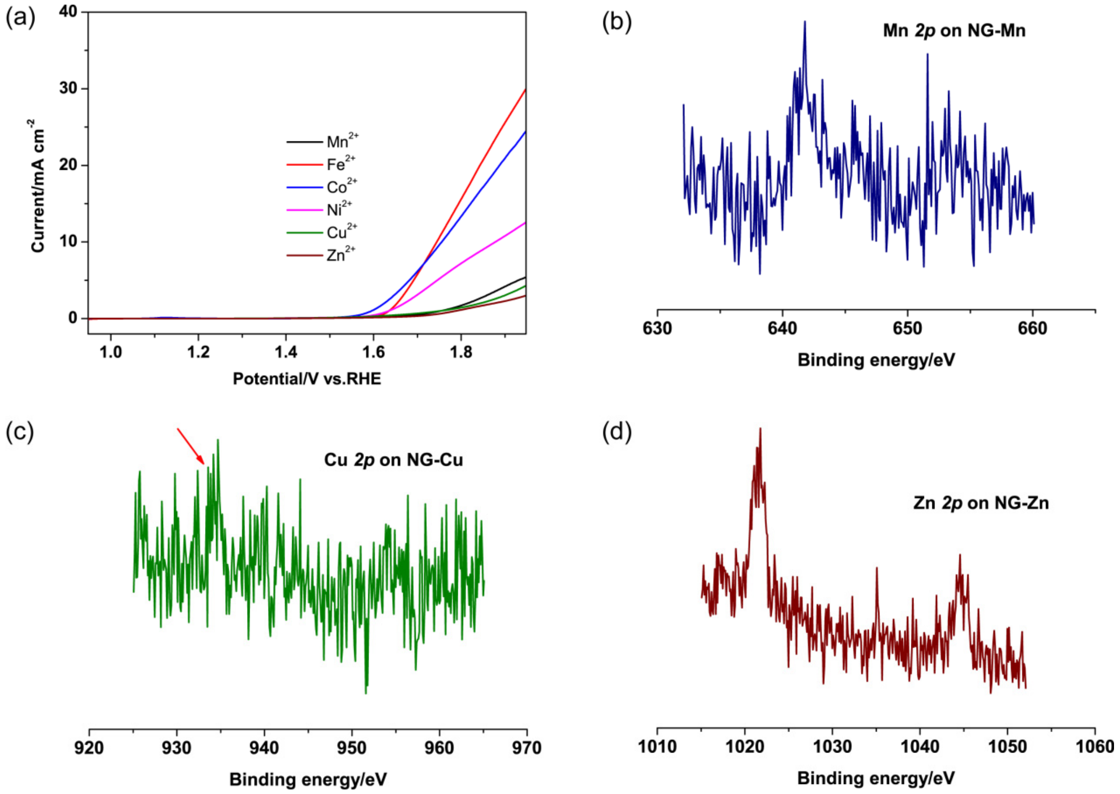

**Figure S1.** (a) OER polarization curves in 0.1 M KOH acquired on NG loaded with different ions: $Mn^{2+}$, $Fe^{2+}$, $Co^{2+}$, $Ni^{2+}$, $Cu^{2+}$, and $Zn^{2+}$ ions, respectively. Rotation speed: 1600 rpm, scan rate: 10 mV $s^{-1}$. XPS spectra of Mn *2p* in NG-Mn (b), Cu *2p* in NG-Cu (c), and Zn *2p* in NG-Zn (d).

The electrocatalysts were synthesized using the same procedures, simply by mixing NG with the $MCl_2$ precursors (M= Mn, Fe, Co, Ni, Cu, and Zn). The NG-Mn, NG-Cu, and NG-Zn samples showed the lowest anodic currents. It could reflect that the loading efficiency of $Mn^{2+}$ and $Cu^{2+}$ ions was poor as indicated by the small XPS signals in Figure S1b and c. However, the Zn signal was relatively clear in the survey of NG-Zn (Figure S1d), which suggested that the intrinsic activity from $Zn^{2+}$ ions was low. Therefore, another possible explanation for the inert OER activity can be that a filling state of *d* orbitals is a general descriptor describing the bond strength between active sites and $HO^-$. Too many (*e.g.*, $Cu^{2+}$ and $Zn^{2+}$ ions) or too few (*e.g.*, $Mn^{2+}$ ions) *d* electrons would make the activation of substrate difficult by insufficient or overly strong chemisorption.[2]

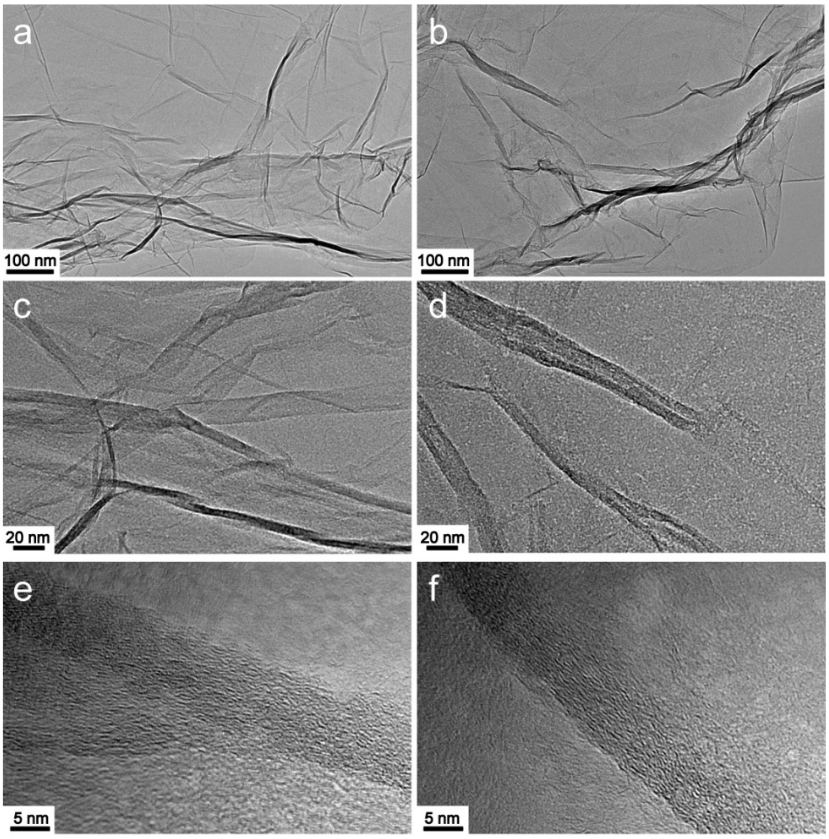

**Figure S2.** Typical TEM images obtained at different magnifications of NG before (a, c, e) and after (b, d, f) immobilizing $Co^{2+}$ ions.

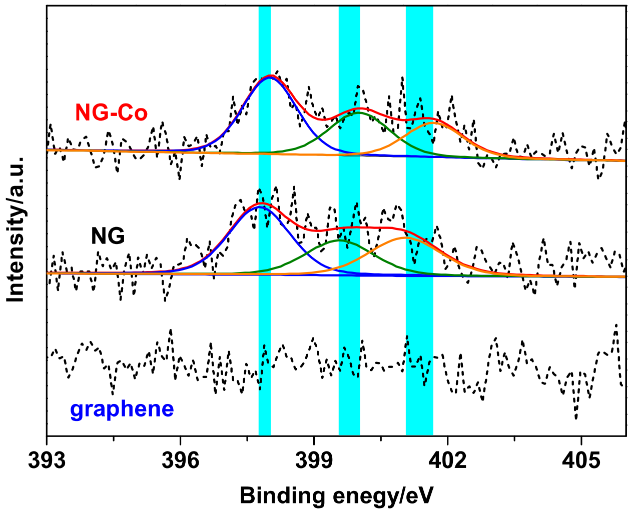

**Figure S3.** XPS survey of N *1s* electron levels in graphene, NG before and after immobilizing $Co^{2+}$ ions.

**Table S1.** Several TOF values reported recently using different catalytic strategies.

| Catalysts source | Electrolyte | Overpotential/V | TOF/$s^{-1}$ |
|---|---|---|---|
| **In this study** | **0.1 M KOH** | **0.40** | **2.53** |
| *ACS. Appl. Interfaces*, **2014**, 5,10172 | 1 M KOH | 0.30 | 0.0024 |
| *J. Am. Chem. Soc.*, **2013**, 135, 17242 | 0.1 M KOH | 0.40 - 0.70 | 0.061-0.88 |
| *Nat. Commun.*, **2014**, 5, 4477 | 1 M KOH | 0.30 | 0.05 |
| *J. Am. Chem. Soc.*, **2013**, 135, 8452 | 1 M KOH | 0.30 | 0.56 |
| *J. Am. Chem. Soc.*, **2010**, 132 16501 | 0.1 M PBS | 0.41 | $2\times10^{-3}$ |
| *Energy Environ. Sci.*, **2013**, 6, 2222 | 2 M KOH | 0.60 | $2.9\times10^{-4}$ |
| *J. Am. Chem. Soc.*, **2013**, 135, 4516 | $Na_2SiF_6$<br>$NaHCO_3$ | Photocatalysis | $2.2\times10^{-3}$ |

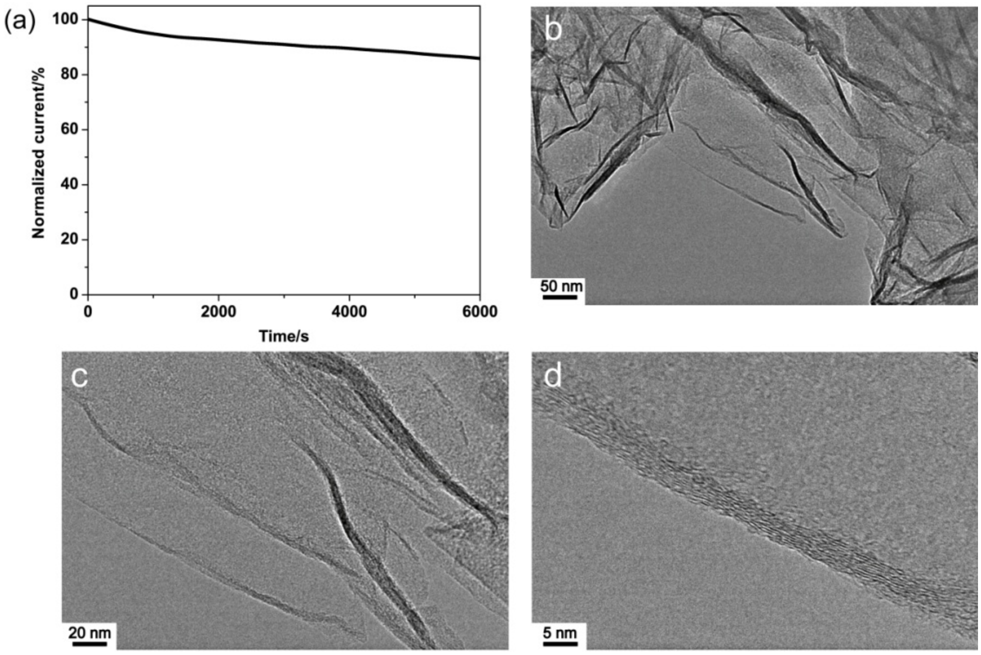

**Figure S4.** (a) Chronoamperometric response (normalized by the starting currents) of OER on NG-Co/GC in 0.1 M KOH at a rotation rate of 1600 rpm. The potential was set at 1.75 *vs.* RHE. (b, c, d) TEM images with different magnifications of NG-Co after the stability test.

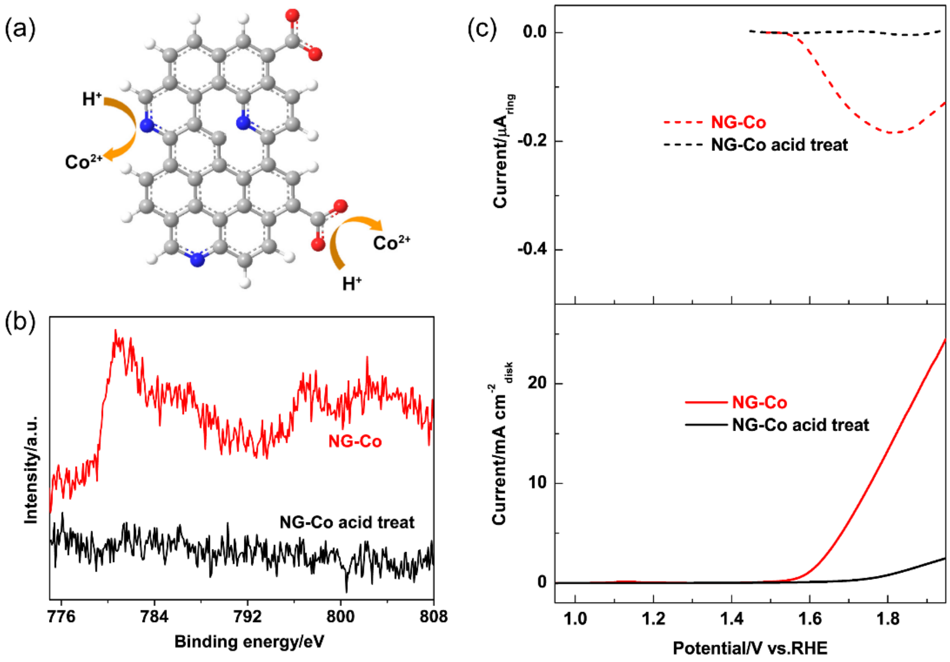

**Figure S5.** (a) Scheme illustrates the detachment of Co$^{2+}$ ions from NG by acid treatment of NG-Co. (b) XPS survey of Co *2p* electrons of NG-Co before and after acid treatment. (c) OER polarization curves (bottom) and corresponding ring current (top) recorded at 1.35 V *vs.* RHE in 0.1 M KOH on Co-NG before and after acid treatment. Rotation speed: 1600 rpm, scan rate: 10 mV s$^{-1}$.

This control experiment was performed to verify the coordination interactions between Co$^{2+}$ ions and NG. Briefly, prior to the test, the NG-Co was treated with 0.5 M $H_2SO_4$ at 80 °C for 12 h to break Co$^{2+}$-N and/or Co$^{2+}$-O bonds. As a result, upon the detachment of active sites from NG, the degradation in OER current occurs. Meanwhile, the cathodic current on the Pt ring became difficult to identify.

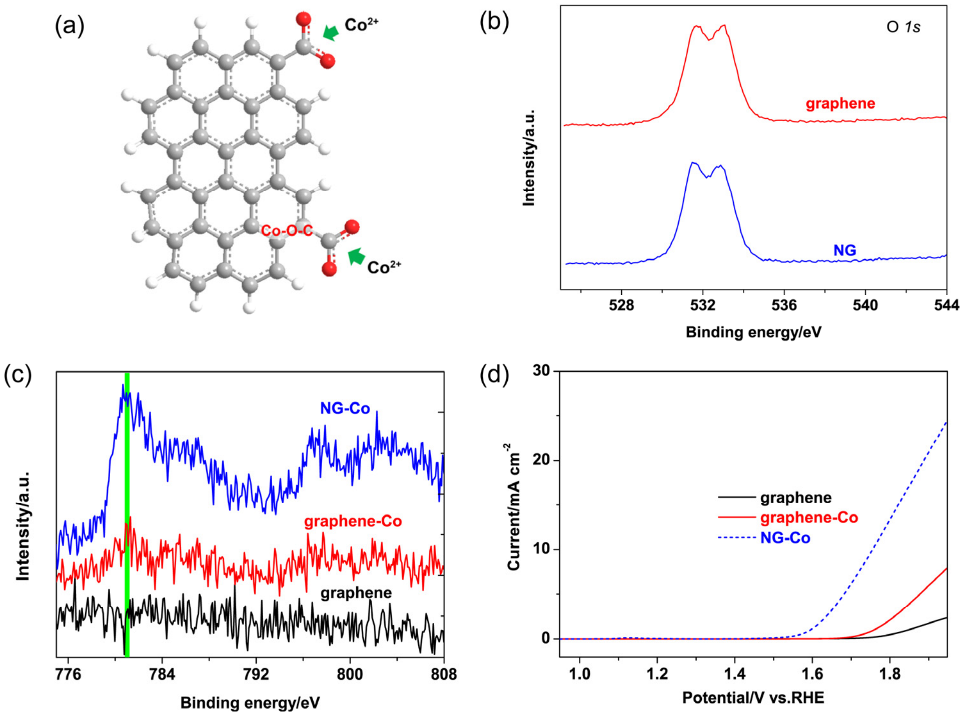

**Figure S6.** (a) Scheme indicates oxygen dopants in graphene driving the formation of graphene-Co. (b) O *1s* survey of NG and graphene. (c) Co *2p* surveys for graphene, graphene-Co and NG-Co. (d) Comparison of OER activities of graphene, graphene-Co and NG-Co in 0.1 M KOH. Rotation rate: 1600 rpm, scan rate: 10 mV $s^{-1}$.

Pyrolysis of GO in the absence of melamine resulted in the formation of graphene, which carries almost the same O-containing groups as in the NG case (Figure S6b). Using the same methodology to synthesize NG-Co, a control sample of graphene-Co was obtained by interacting graphene with $Co^{2+}$ ions. However, weaker Co *2p* signals collected on the sample suggested that these O-containing groups had lower affinity to $Co^{2+}$ ions comparing to the N dopants (Figure S6c). Although improvement of OER activity was observed on graphene-Co, it was not comparable to NG-Co as revealed by both overpotential and current density. These results implied that the N doping strategy can support more amount active sites within graphene, as well as leads to a more favorable adsorption for $HO^{-}$ on Co-N.

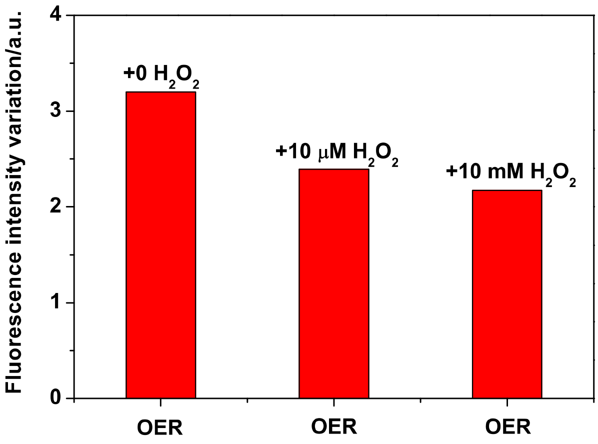

**Figure S7.** The fluorescence intensity variation from hydroxylation of coumarin during OER over NG-Co/GCE at 1.65 V *vs.* RHE for 50 min in 0.01 M KOH containing 0, 10 μM and 10 mM $H_2O_2$, respectively. The KOH solution was diluted to avoid hydrolysis of coumarin.

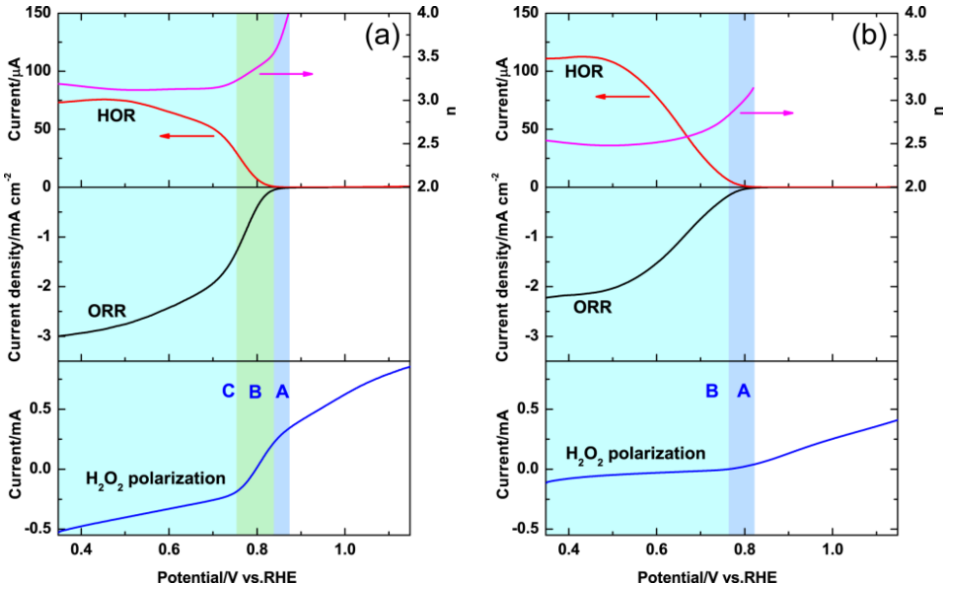

**Figure S8.** The ORR polarization curves acquired on NG-Co (a) and NG (b) in 0.1 M KOH, the corresponding $H_2O_2$ oxidation current on the Pt ring was recorded at 1.35 V and the derived *n* values were summarized. Rotation speed: 1600 rpm; Scan rate: 10 mV s$^{-1}$. Under the same conditions, the polarization of 6 mM $H_2O_2$ on NG and Co-NG was performed in 0.1 M KOH under $N_2$ atmosphere protection (bottom) at a rotation speed of 1600 rpm, and a scan rate of 10 mV s$^{-1}$.

The potentials lower than the standard potential of $E^{0'}(O_2/H_2O)$ were applied on the NG-Co/GC for evaluating the electrocatalytic activity for oxygen reduction reaction (ORR). In 0.1 M KOH, the polarization curves in RRDE measurements (Figure S8) showed that the NG-Co catalyst exhibited higher cathodic current with lower overpotential than NG, which demonstrated that the immobilized $Co^{2+}$ ions also facilitated the *4e*-transfer ORR. Either direct or indirect *4e*-transfer reaction indicated that the electrocatalyst had the stronger capability to break O=O double bond as compared to *2e*-transfer of ORR. Within the potential range of ORR, the redox behavior of $H_2O_2$ on NG-Co and NG was compared. It can be seen clearly that NG-Co could effectively activate $H_2O_2$, showing a significant cathodic current as compared to the one obtained on NG. When certain amount of $H_2O_2$ was formed in the ORR on NG-Co, its redox contributed to the higher apparent electron transfer number (*n*) and cathodic current at the disk electrode.

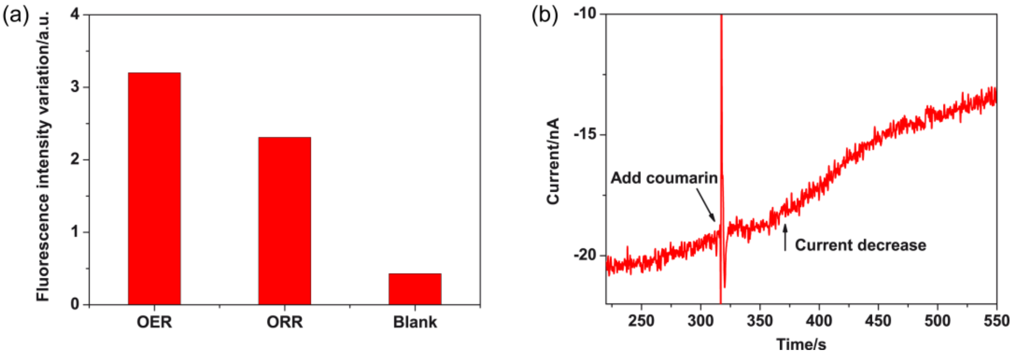

**Figure S9.** (a) Comparison of fluorescence emission after ORR and OER on NG-Co/GCE at 0.75 V *vs.* RHE and 1.65 V *vs.* RHE in 0.01 M KOH containing 60 μM coumarin for 50 min, respectively. The blank signal was obtained from a control experiment performed under the same conditions but without applying potential. (b) Current-time curve for ORR at 0.8 V *vs.* RHE in air saturated 0.01 M KOH (water/ethanol as solvent, 1:1 V/V). The ORR current jumped at 315 s which represented the injection of 0.6 mM coumarin into the electrolyte, afterwards it showed a gradual decrease.

As revealed by the *in situ* fluorescence spectroelectrochemistry measurements, the continuous running of ORR on NG-Co catalyst at 0.75 V *vs.* RHE also resulted in fluorescence emission at 500 nm, demonstrating the formation of fluorescent 7-hydroxyl-coumarin since there appeared only a relatively weaker fluorescence emission of the mixture of coumarin and KOH electrolyte at open circuit potential for the same time period (Figure S9a). Under ambient environments, the solubility of oxygen in KOH solution was relatively low (less than $10^{-3}$ M). It was observed that the cathodic current on NG-Co/GC gradually decreased in air-saturated KOH upon addition of more amount of coumarin (0.6 mM), which demonstrated the intermediate nature of $HO^{\bullet}$ in ORR (Figure S9b). Therefore, the process forming $HO^{\bullet}$ should be the main elemental step for 4e-transfer of ORR ($HO^{\bullet} + e \rightarrow HO^{-}$, $E^0 = 1.9$ V *vs.* NHE)[3], although the side pathway to generate $HOO^{-}$ as byproduct could not be excluded.

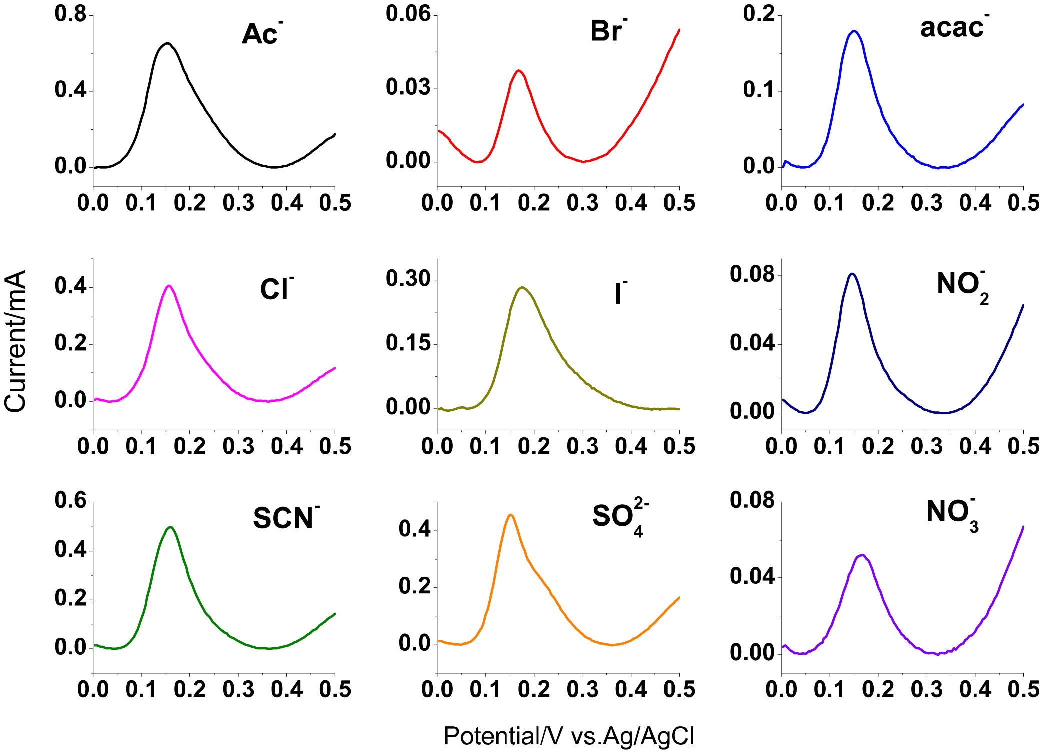

**Figure S10.** Differential pulse voltammograms (DPVs) of NG-Co-L prepared from cobalt salts with different counter anions. Amplitude: 50 mV; Pulse period: 0.2 s; Electrolyte: 0.1 M KOH. The Y-axis stands for the DPV current/mA and X-axis is potential *vs.* Ag/AgCl.

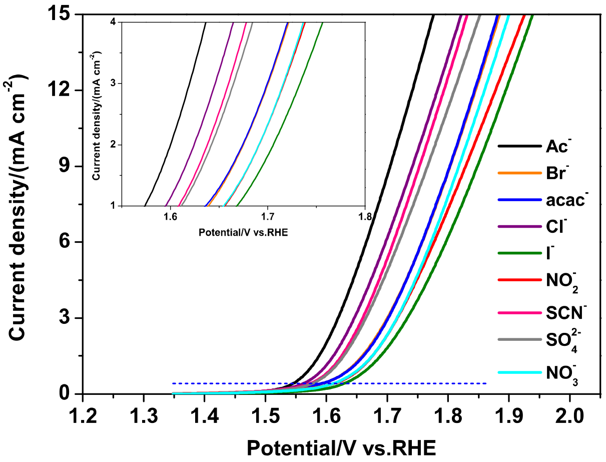

**Figure S11.** OER polarization curves obtained on NG-Co-L. Rotation speed: 1600 rpm, scan rate: 10 mV $s^{-1}$; Electrolyte: 0.1 M KOH.

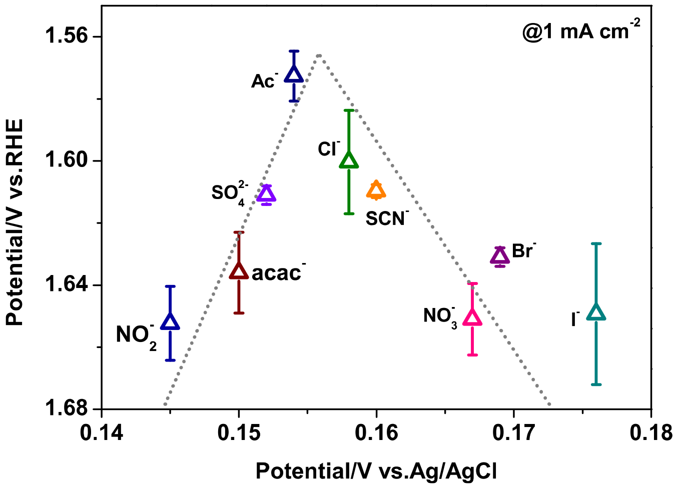

**Figure S12.** OER potentials required on NG-Co-L catalysts at 1 mA cm$^{-2}$ as a function of anodic potentials of the immobilized Co$^{2+}$ ions.

## References

1. J. Wang, K. Wang, F.-B. Wang and X.-H. Xia, *Nat. Commun.*, 2014, 5.

2. J. Suntivich, K. J. May, H. A. Gasteiger, J. B. Goodenough and S. H. Yang, *Science*, 2011, 334, 1383-1385.

3. J. M. Noël, A. Latus, C. Lagrost, E. Volanschi and P. Hapiot, *J. Am. Chem. Soc.*, 2012, 134, 2835-2841.